Materials Letters 64 (2010) 1858–1860

Contents lists available at ScienceDirect

Materials Letters

journal homepage: www.elsevier.com/locate/matlet

# Morphologically controlled synthesis of mesoporous alumina using sodium lauroyl glutamate surfactant

Fei Xiu, Wei Li *

*Key Laboratory of Advanced Energy Materials Chemistry (Ministry of Education), College of Chemistry, Nankai University, Tianjin, 300071, China*

ARTICLE INFO

*Article history:*
Received 24 March 2010
Accepted 14 May 2010
Available online 31 May 2010

*Keywords:*
Surfactant
Porosity
Nanomaterials

ABSTRACT

Mesoporous alumina with various morphologies has been successfully synthesized by a proper sol–gel process using sodium lauroyl glutamate surfactant as a template. Both the mesostructures and morphologies of the resulting alumina can be effectively controlled by adjusting the concentration of the sodium lauroyl glutamate surfactant present in the reaction system. Through characterization by X-ray diffraction, transmission electron microscopy, and $N_2$ physisorption, the effects of sodium lauroyl glutamate on the mesostructure and morphology of the resulting materials have been investigated in detail, and a possible formation mechanism of the controlled morphologies is proposed. The resulting mesoporous materials showed a potential application in adsorption of toxic organic compounds, which was attributed to the porous structure, high BET surface area, and large pore volume.



## 1. Introduction

Morphologically controlled synthesis of mesoporous alumina (MA) has received much attention recently because morphology is an important factor influencing the properties and applications of alumina materials, in addition to specific surface area and pore size distribution. Studies focusing on the synthesis of mesoporous silica with various morphologies indicate that the morphologies of mesoporous materials might be controlled through modification of the inorganic/organic interactions by adjusting the synthesis conditions [1,2]. Liu et al. have reported the morphologically controlled synthesis of MA by a hydrothermal synthesis route using $Al(NO_3)_3$/$NH_3$/urea/surfactant as reactants [3]. In their work, by adjusting the synthesis conditions such as reactant compositions, hydrothermal time, and surfactant types, MA samples in the regular form of spheres, rods, fibers, and unique three-dimensional dumbbell, flower-like hierarchical architectures were obtained for the first time.

There are lots of reports on the sol–gel synthesis of MA [4–6]. In this work, we report a new method for the simple and effective synthesis of MA with various mesostructures and morphologies using sodium lauroyl glutamate (LAG-Na) as a novel type of template according to a proper sol–gel method. MA materials with wormhole framework structure and hollow spherical structure with mesochannels on the shell were successfully synthesized by adjusting the concentration of LAG-Na present in the reaction system. A possible formation mechanism for the controlled morphologies is proposed, and application of the resulting materials in adsorption was characterized.

To the best of our knowledge, this is the first report on the use of this salt as a template and this method in the synthesis of hollow alumina nanospheres.

## 2. Experiments

### 2.1. Synthesis of MA materials

All of the chemicals used in the experiments were AR grade, and were used without further purification.

LAG-Na (5.82 g) was dissolved in 40 mL of deionized water at 35 °C. Sodium aluminate (1.4 g) was added to the polymer solution with stirring for 30 min. Then hydrochloric acid was added dropwise until the pH of the solution was 7. The mixture was left at 35 °C for 5 h under stirring and then transferred to an oven at 100 °C for 16 h under quiescent conditions. The final white product was filtered, washed with deionized water, and dried at 120 °C. To obtain the pure MA without the surfactant, we calcined the as-synthesized samples at 600 °C for 3 h. A constant 1/1 surfactant/Al mole ratio was always used, and the morphology adjustment was achieved by changing the surfactant/water mole ratio.

### 2.2. Adsorption experiments

The adsorption isotherm experiments of benzene onto alumina were performed on the basis of a batch experiment. A given amount of adsorbent (0.05 g) was placed in a 50 mL flask, to which a benzene solution (25 mg/L) was added. The experiments were performed in a

* Corresponding author.
*E-mail address:* weili@nankai.edu.cn (W. Li).

0167-577X/$ – see front matter © 2010 Elsevier B.V. All rights reserved.
doi:10.1016/j.matlet.2010.05.027

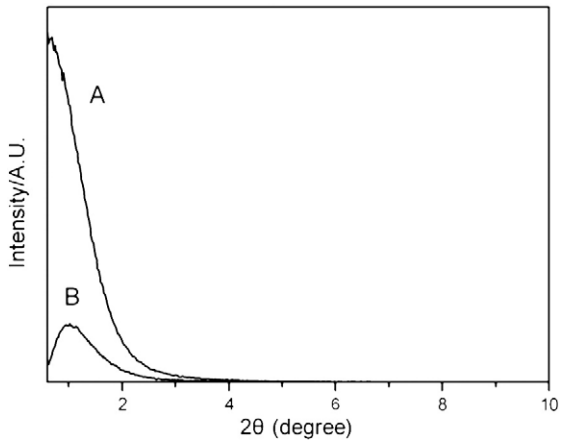


**Fig. 1.** Small-angle XRD patterns of MA after calcination at 600 °C: A (concentration of surfactant of 0.1 mol/L), B (concentration of surfactant of 0.4 mol/L).

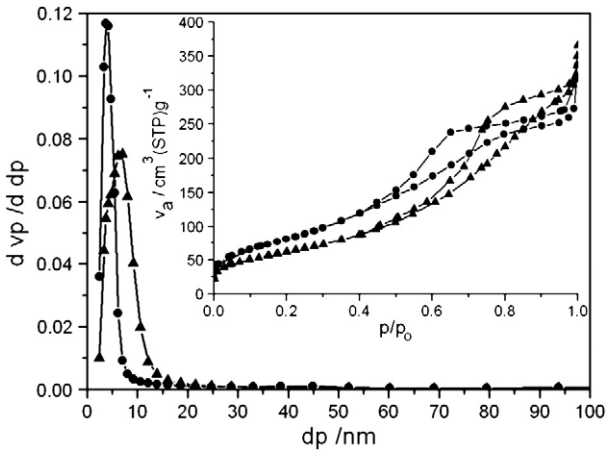


**Fig. 3.** $N_2$ adsorption–desorption isotherms and pore size distributions of samples: ▲ sample A; ● sample B.

temperature-controlled water bath shaker for 2 h at a shaking speed of 180 rpm. After the adsorption reached equilibrium, the solutions were filtered and analyzed for the remaining concentration of benzene.

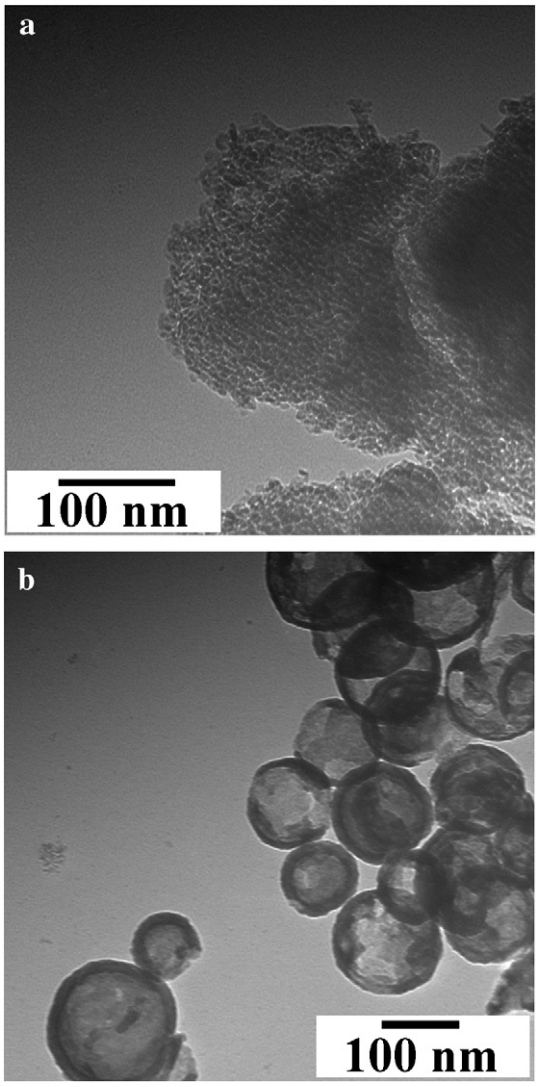


**Fig. 2.** (a) TEM image of sample A; (b) TEM image of sample B.

The specific amount of benzene adsorbed was calculated using Eq. (1) as follows:

$$q_e = (C_0 - C_e) \times V / W \quad (1)$$

where $q_e$ is the adsorption capacity (mg/g) of the solid at equilibrium; $C_0$ and $C_e$ are the initial and equilibrium concentrations of solute (mg/L), respectively; $V$ is the volume of the aqueous solution (L); and $W$ is the mass (g) of adsorbent used in the experiments.

### 2.3. Characterization

Powder X-ray diffraction was performed on a Rigaku D/Max-2500 diffractometer, with Cu Kα at 40 kV and 100 mA. Transmission electron microscopy (TEM) images were acquired using a JEOL-2010 FEF high-resolution transmission electron microscope. The surface area (BET), pore size distribution, and pore volume were determined by nitrogen adsorption at − 196 °C using an automated gas adsorption analyzer (BELSORP-mini, Holland). The concentration of benzene was analyzed using a UV-spectrophotometer (Model-UV2100) at a wavelength of 245 nm.

## 3. Results and discussion

### 3.1. The structural properties of the samples

Small-angle XRD patterns of the samples are shown in Fig. 1. It can be seen that sample A did not show any XRD peaks in the small-angle region. Even for sample B, prepared with a concentration of surfactant of 0.4 mol/L, only one small-angle peak at $2\theta$ approximately equal to 1° was observed, which indicated the presence of mesoporous materials with no long-range order pore structure [7].

Fig. 2a shows the TEM image of sample A obtained with the concentration of surfactant equal to 0.1 mol/L with typical wormhole framework structure. There is no long-range order in the pore arrangement, which is in good agreement with the result of small-angle XRD. The micrograph shows that the channels of sample B are not regular in diameter, which corresponds well with the BJH

**Table 1**
Selected synthetic parameters and physical properties of the MA after calcination.

| Sample | Concentration of surfactant (mol/l) | Surface area ($m^2$/g) | Volume ($cm^3$/g) | BJH pore size (nm) |
|---|---|---|---|---|
| A | 0.1 | 230 | 0.55 | 7.1 |
| B | 0.4 | 268 | 0.45 | 3.7 |


**Scheme 1.** Schematic illustration for the formation process of the hollow alumina mesoporous nanospheres.

isotherm. MA prepared with a higher concentration of surfactant shows a quite different spherical morphology, as shown in Fig. 2b. The hollow spheres have a uniform shell with a thickness of 13–15 nm and inner cavities with diameters mostly in the range of 70–120 nm. Fig. 2b clearly demonstrates that the alumina samples with regular hollow spherical morphology consisted of mesopores, which is in good agreement with the results of $N_2$ physisorption and the small-angle XRD pattern.

From Fig. 3, it can be seen that all of the samples showed type-IV (IUPAC) isotherms, pointing to mesoporous materials [8]. The hysteresis loop at low relative pressure was due to capillary condensation of the filling nitrogen in the mesopores. The pore size distributions and the structure parameters demonstrated the significant role of the concentration of the surfactant. Samples A and B showed narrow pore size distributions centered at 7.1 nm and 3.7 nm pore diameter, respectively (Fig. 3). In sample A, prepared with a lower concentration of LAG-Na, the pore size distribution was much broader, characteristic of a disordered sample [9]. Table 1 shows that sample B displays a high surface area of 268 $m^2/g$ and pore volume of 0.45 $cm^3/g$, and sample A prepared with a lower concentration of surfactant had lower BET surface areas. Furthermore, our experimental results showed that the specific surface area, pore volume, and pore size could be fine-tuned by changing the concentration of the surfactant of the starting solution.

In the present study, the concentration of LAG-Na surfactant is shown to have an important effect on the mesostructures and morphologies of the resulting alumina materials. Here is a possible formation mechanism: In the initial solution, the LAG-Na surfactant at a high concentration formed strong micelles through the directional arraying of the hydrophilic and hydrophobic groups. As the sodium aluminate hydrolyzed in the acid solution, aluminum hydroxide was formed and precipitated from the solution [10]. The fresh precipitate was electropositive and could interact with surfactant micelles. Such interactions might play a significant role in directing the mesophase formation, and the strong surfactant micelles acted as a solid core in the formation of the shell. The surfactant decomposed completely upon calcination at 600 °C, and the carbon dioxide as well as water generated was released, which resulted in the porosity of the shells and formation of the hollow structures. A related schematic illustration for the formation process of the hollow alumina mesoporous nanospheres is shown in Scheme 1. When the concentration of surfactant decreased, the morphology of the resulting alumina changed from mesoporous hollow spheres to wormhole-like mesoporous structures. A possible reason is as follows: In the case of insufficient surfactant, the surfactant micelles were not strong enough to offer a solid core, leading to failure to form hollow spheres upon calcination. Through the calcination treatment, wormhole framework structures were formed because of the release of carbon dioxide and water from the system.

### 3.2. Adsorption application of samples

Adsorption of benzene onto MA materials synthesized in this work was studied, and compared with that onto commercial MA (Supplementary material, Table 2). The results showed that the adsorption capabilities of the synthesized alumina materials were higher than those of commercial alumina and could be attributed to porous structure, high surface area, and large pore volume of the adsorbent.

## 4. Conclusions

We have reported a simple and effective sol–gel process using LAG-Na surfactant to synthesize MA materials with different morphologies. MA materials with wormhole framework structure and hollow spherical structure with mesochannels on the shell were successfully synthesized by adjusting the concentration of LAG-Na. It is considered that LAG-Na surfactant micelles play different roles in reaction systems with different concentrations of LAG-Na, resulting in various morphologies of the resulting products. The described method provides alumina materials with good porosity and has potential for applications in the adsorption field.

## Acknowledgements

The authors acknowledge financial support from the Research Fund for the Doctoral Program of Higher Education (20090031110015), and the Program for New Century Excellent Talents in University (NCET-10-0481).

## Appendix A. Supplementary data

Supplementary data associated with this article can be found, in the online version, at doi:10.1016/j.matlet.2010.05.027.

## References

[1] Zhao DY, Yang PD, Huo QS, Chmelka BF, Stucky GD. Curr Opin Solid State Mater Sci 1998;3:111.
[2] Lin HP, Mou CY. Acc Chem Res 2002;35:927–35.
[3] Liu Q, Wang A, Wang X, Zhang T. Microporous Mesoporous Mater 2007;100:35–44.
[4] Aguado J, Escola JM, Castro MC, Paredes B. Microporous Mesoporous Mater 2005;83:181–92.
[5] Niesz K, Yang PD, Somorjai GA. Chem Commun 2005:1986–7.
[6] Yao N, Xiong GX, Zhang YH, He MY, Yang WS. Catal Today 2001;68:97–109.
[7] Naděžda Žilková, Arnošt Zukal, Jiří Čejka. Microporous Mesoporous Mater 2006;95:176–9.
[8] Xu B, Xiao T, Yan Z, Sun X, Sloan J, González-Cortés SL, et al. Microporous Mesoporous Mater 2006;91:293–5.
[9] Yada M, Hiyoshi H, Machida M, Kijima T. J Porous Mater 1998;5:133–8.
[10] Wang JG, Li F, Zhou HJ. Chem Mater 2009;21:612–20.